stronger near the trailing edge of the moving pattern, revealing an imbalance in motion processing at the trailing and leading edges.

In the first experiment, the patterns containing motion were blurry (Fig. 1). However, if there is a mechanism that operates more strongly at the trailing edge or origin of motion in these patterns, it should operate whether or not the patterns are blurry. We thus conducted an experiment identical to the first, except that the patterns were given a hard aperture rather than a blurry luminance profile (Fig. 4A). The illusory position shift is reduced or eliminated in these sharp-edged patterns (*1*, *2*). The pattern of activation, however, was identical to that in the first experiment (Fig. 4A). Therefore, the pattern of activation is not specific to a visual illusion, but to the trailing edges or origin of the motion.

If there is a mechanism that selectively operates on the trailing edges of moving patterns, it should operate irrespective of whether a shift in the position of the pattern is perceived: This is precisely what we found. The bias in the retinotopic representation of the pattern is consistent in both this experiment and the first one. The peak activity always occurred near the trailing edge, no matter where the patterns were perceived (compare Figs. 2 and 4). Clearly, activity in the visual cortex, as revealed by fMRI, does not necessarily correlate with shifts in perceived position.

All of the stimuli described thus far have been symmetrically moving patterns—either toward or away from the fovea. Is it possible that the optic flow in these stimuli was responsible for the results? In an additional experiment, using stimuli that did not contain expanding or contracting optic flow, we presented segments of a windmill pattern that moved either toward or away from each other (Fig. 4B and fig. S6). Although there is no clear optic flow in this stimulus, the pattern of activation was identical to that in the previous experiments: Peak activation always occurred near the trailing edge of the moving patterns.

The experiments presented here clearly demonstrate that the representation of position, even in early visual cortical areas such as V1, depends on motion signals that are present in a scene. The imaging and psychophysical results revealed a mechanism that operates selectively on the trailing edges of moving stimuli. More important, the results demonstrated a clear dissociation: fMRI activation did not correlate with what subjects perceived, showing that the BOLD response is not a necessary correlate of perception.

References and Notes

1. R. L. De Valois, K. K. De Valois, *Vision Res.* **31**, 1619 (1991).
2. V. S. Ramachandran, S. M. Anstis, *Perception* **19**, 611 (1990).
3. S. Nishida, A. Johnston, *Nature* **397**, 610 (1999).
4. R. J. Snowden, *Curr. Biol.* **8**, 1343 (1998).
5. D. Whitaker, P. V. McGraw, S. Pearson, *Vision Res.* **39**, 2999 (1999).
6. D. Whitney, P. Cavanagh, *Nature Neurosci.* **3**, 954 (2000).
7. Stimuli not shown.
8. Materials and methods are available as supporting material on *Science* Online.
9. V. A. Lamme, B. W. van Dijk, H. Spekreijse, *Nature* **363**, 541 (1993).
10. J. B. Reppas, S. Niyogi, A. M. Dale, M. I. Sereno, R. B. Tootell, *Nature* **388**, 175 (1997).
11. P. M. Daniel, D. Whitteridge, *J. Physiol.* **159**, 203 (1961).
12. M. I. Sereno *et al.*, *Science* **268**, 889 (1995).
13. R. B. Tootell, M. S. Silverman, E. Switkes, R. L. De Valois, *Science* **218**, 902 (1982).
14. R. B. Tootell *et al.*, *Proc. Natl. Acad. Sci. U.S.A.* **95**, 811 (1998).
15. P. P. Battaglini, C. Galletti, P. Fattori, *Arch. Ital. Biol.* **131**, 303 (1993).
16. V. Virsu, J. Rovamo, *Exp. Brain Res.* **37**, 475 (1979).
17. J. R. Wilson, S. M. Sherman, *J. Neurophysiol.* **39**, 512 (1976).
18. D. C. Somers, A. M. Dale, A. E. Seiffert, R. B. Tootell, *Proc. Natl. Acad. Sci. U.S.A.* **96**, 1663 (1999).
19. R. B. Tootell *et al.*, *Neuron* **21**, 1409 (1998).
20. J. A. Brefczynski, E. A. DeYoe, *Nature Neurosci.* **2**, 370 (1999).
21. P. Cavanagh, *Science* **257**, 1563 (1992).
22. F. A. Verstraten, P. Cavanagh, A. T. Labianca, *Vision Res.* **40**, 3651 (2000).
23. M. J. Berry II, I. H. Brivanlou, T. A. Jordan, M. Meister, *Nature* **398**, 334 (1999).
24. P. J. Bex, G. K. Edgar, A. T. Smith, *Vision Res.* **35**, 2539 (1995).
25. Y. X. Fu, Y. Shen, Y. Dan, *J. Neurosci.* **21**, RC172 (2001).
26. M. A. Georgeson, S. T. Hammett, *Proc. R. Soc. Lond. Ser. B* **269**, 1429 (2002).
27. V. S. Ramachandran, V. M. Rao, T. R. Vidyasagar, *Perception* **3**, 97 (1974).
28. S. F. Stasheff, R. H. Masland, *J. Neurophysiol.* **88**, 1026 (2002).
29. D. Burr, *Nature* **284**, 164 (1980).
30. K. Kirschfeld, T. Kammer, *Vision Res.* **39**, 3702 (1999).
31. J. Müsseler, G. Aschersleben, *Percept. Psychophys.* **60**, 683 (1998).

32. We thank G. Alvarez, D. Arnold, P. Cavanagh, A. Johnston, A. Kuchinad, B. Macintosh, P. Martini, I. Murakami, S. Nishida, E. Veinsreideris, T. Vilis, and T. Watanabe. This work was supported by NIH and the Canadian Institutes of Health Research.

Supporting Online Material

www.sciencemag.org/cgi/content/full/302/5646/878/DC1
Materials and Methods
Figs. S1 to S8
References

10 June 2003; accepted 15 July 2003.

Optical Imaging of a Tactile Illusion in Area 3b of the Primary Somatosensory Cortex

Li M. Chen,[1] Robert M. Friedman,[2] Anna W. Roe[1]*†

In the tactile funneling illusion, the simultaneous presentation of brief stimuli at multiple points on the skin produces a single focal sensation at the center of the stimulus pattern even when no physical stimulus occurs at that site. Consistent with the funneling percept, we show with optical imaging in area 3b of the primary somatosensory cortex (SI) that simultaneous stimulation of two fingertips produces a single focal cortical activation between the single fingertip activation regions. Thus, in contrast to traditional views of the body map, topographic representation in the SI reflects the perceived rather than the physical location of peripheral stimulation.

The key aspect of the tactile funneling illusion is the illusory perception of skin stimulation at a single site central to an actual line of multiple stimulation sites (*1*–*5*). Inputs at lateral sites are "funneled" centrally so that the perceived intensity at the central site is greater than that perceived to stimulation at the middle site alone. With two-point stimulation, a funneled sensation is produced at a central location that is not directly stimulated (*1*, *3*, *4*). This illusion has been reported on the forearm, palm, and fingers. Thus, the funneling illusion is characterized by a perception of spatial mislocalization and increased tactile intensity.

How is a mislocalized sensation encoded in the brain? Previous studies have shown that the funneling illusion is encoded in the primary somatosensory cortex (SI) and not peripherally at the skin (*2*). The responses of SI neurons to three-point skin stimulation have demonstrated that a broad distribution of cortical neurons are recruited (*6*, *7*). However, it is unknown which of the SI areas (areas 3a, 3b, 1, or 2) are involved in funneling and at what stage the funneling is first encoded. Furthermore, the SI is topographically organized, but it is unknown whether the somatotopy is founded on a physical map or a perceptual map. The funneling illusion may provide an answer to whether cortical activation corresponds to the actual or perceived site of peripheral stimulation.

[1]Department of Neurobiology, Yale University School of Medicine, New Haven, CT 06520, USA. [2]Department of Anesthesiology, Yale University School of Medicine, New Haven, CT 06520, USA.

*To whom correspondence should be addressed. E-mail: anna.roe@vanderbilt.edu
†Present address: Department of Psychology, Vanderbilt University, 066 Wilson Hall, 111 21st Avenue South, Nashville, TN 37203, USA.

To study this mislocalization percept, we used intrinsic-signal optical imaging, a method that detects stimulus-specific neural responses by measuring changes in cortical reflectance correlated with blood oxygenation levels (*8*). In the squirrel monkey, optical imaging has been used to demonstrate that single-digit stimulation [in digits D1 (thumb) to D5 (little finger)] produces discrete, focal activations in area 3b, consistent with small single-digit receptive fields found in area 3b, and that these activations are arranged from lateral to medial in the expected topographic order (*9*, *10*). For the funneling illusion, we predicted that simultaneous stimulation of two digits would produce one of three response patterns in area 3b: (i) two focal cortical activation spots corresponding to stimulated digits, (ii) a broad region of activation encompassing both regions of digit stimulation, or (iii) a single focal activation spot that is central to stimulated digits in parallel with the psychophysical funneling illusion. In addition, we studied the amplitude of the optical response as a possible basis for encoding the heightened intensity of the funneling percept.

We used a paired indentation of probes (3 mm in diameter) on the fingerpads to elicit the funneling sensation. We confirmed psychophysically in humans that our stimulation paradigm produced the funneling percept (*11*). We then used the same stimuli to elicit activations in the cortex of anesthetized squirrel monkeys that were monitored with optical imaging methodology (*10*, *11*). Two cases are shown in Fig. 1. In both case 1 (left) and case 2 (right), stimulation of either D2 alone (Fig. 1, A and B), D3 alone (Fig. 1, C and D), or D4 alone (Fig. 1, E and F) elicited single-focal millimeter-sized activations. The locations of these spots (D2, pink; D3, yellow; D4, green) were consistent with the known digit topography in area 3b and corresponded to the topographic locations of D2, D3, and D4 as determined electrophysiologically (Fig. 1M, dotted lines). Simultaneous stimulation of nonadjacent digits D2 and D4 together (Fig. 1, I and J) produced two separate activation spots in approximately the same locations as the single-digit activations (Fig. 1N). In contrast, stimulation of adjacent digits D3 and D4 (Fig. 1, G and H) produced a single activation site with a center located between the D3 and D4 sites (Fig. 1L).

In all of the cases examined (five adjacent-digit pairs and four nonadjacent-digit pairs), we obtained similar patterns of activation. Figure 1O plots the locations of activation spots resulting from paired-digit stimulation (activations numbered by case). A merging index (MI) was designed to measure the spatial shift in the activation-spot location. The MI ranges from –1 (cortical location of one digit) to 0 (center between two digits) to 1 (cortical location of the other digit). Under two-digit stimulation conditions, the center of digit activation can shift toward the center ($|MI| < 1$) or away from the center ($|MI| > 1$). For all adjacent-digit pairs (four D3+D4 pairs and one D2+D3 pair), stimulation resulted in single activation sites (Fig. 1O, red numbers, top) located between the two single-digit activations [Fig. 1P, MI = 0.54 ±

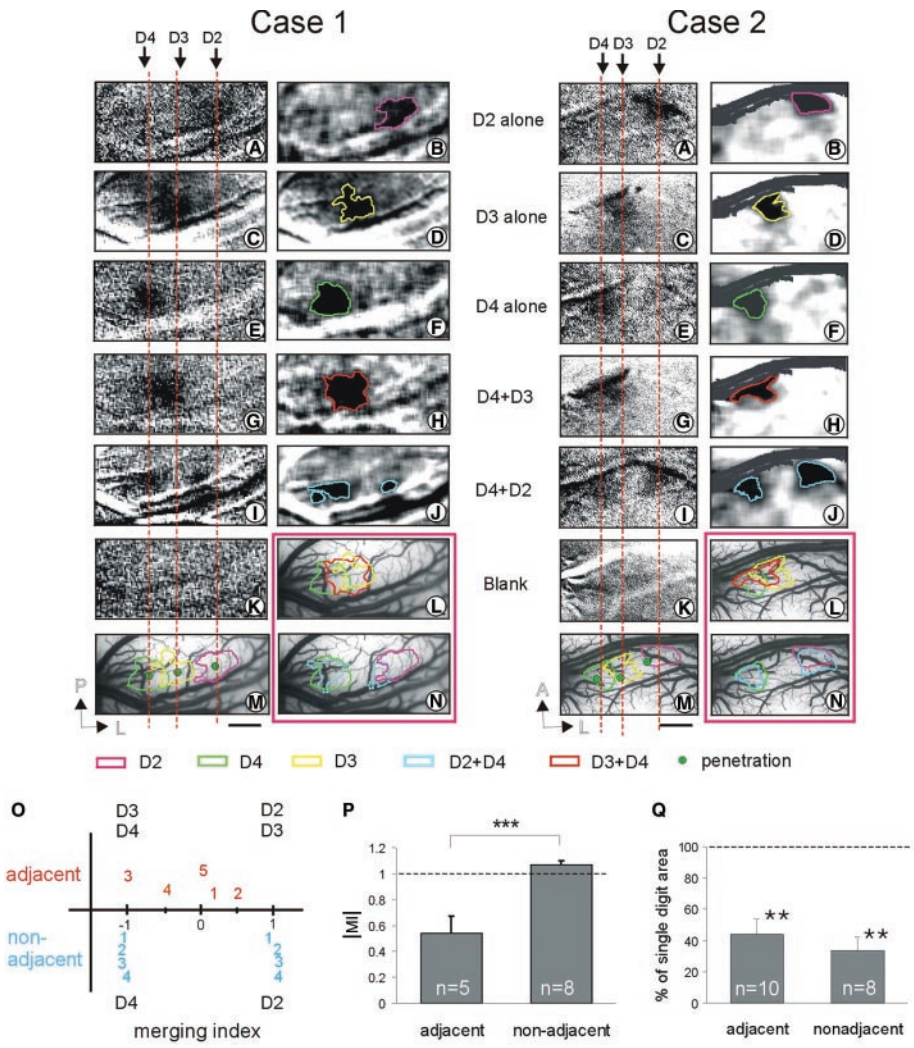

Fig. 1. Imaged activations in area 3b evoked by single-digit (D2, D3, and D4) and paired-digit (D3+D4 and D2+D4) stimulation. Two cases are shown. For each case, raw images are shown in the left column (**A**, **C**, **E**, **G**, and **I**) and low-passed images are shown in the right column (**B**, **D**, **F**, **H**, and **J**). Centers of single-digit activations are indicated by red dashed lines. (**K**) Blank condition. (**L** to **N**) Overlay of outlines of adjacent-digit (L), single-digit (M), and nonadjacent-digit (N) activations. (M) Locations of neurons with D2, D3, and D4 receptive fields (green dots). P, posterior; L, lateral; A, anterior. (**O**) Position of activation centers (on the MI scale) that occurred after paired stimulation of adjacent-digit (top, red numbers, $n = 5$) and nonadjacent-digit (bottom, blue numbers, $n = 4$) stimulation. Half as many points are plotted for adjacent digits, because adjacent-digit stimulation results in only one activation spot. Numbers indicate case number. (**P**) Mean value of |MI|s. (**Q**) Percentage decrease in activation area at single-digit locations compared to corresponding two-digit activation area. Scale bar, 1 mm. *t* test: **, $P < 0.01$; ***, $P < 0.001$. Error bars show the SEM.

0.13 (mean ± SEM)]. In one case (indicated by the red 3), the single activation site was shifted toward one of the digit locations (case 3, MI = 1.0). In contrast, all four nonadjacent digit–pair stimulations (four D2+D4 pairs) resulted in two focal activation sites, each of which was similar in location to the single-digit activation sites (Fig. 1O, blue numbers, bottom; Fig. 1P, mean MI = 1.07 ± 0.03). To further quantify the significance of the shift of activation, we used a discriminability index (D′), which is a measure of the separation relative to the spread of activations (*11*). A low D′ between single- and two-digit activation spots indicates a small shift, and a high D′ indicates a large shift. The mean D′ of all nonadjacent-digit comparisons (n = 8) was 0.017 ± 0.51, whereas the mean D′ of all adjacent-digit comparisons (n = 8) was 0.69 ± 0.21, which was significantly greater than a D′ of 0 (no change, one sample t test $P < 0.001$). These two groups were significantly different ($P < 0.02$). Thus, adjacent-digit stimulations produced significantly greater shifts in activation than those produced by nonadjacent-digit stimulations. This is consistent with the observation that the illusory percept is dependent on the distance between stimulation sites.

Another characteristic of multipoint stimulation (two or more points) is an increased intensity of the funneled sensation in comparison to stimulation at a single site. Responses of single cortical neurons to multipoint stimulation are often similar in magnitude to single-point stimulation (*6*). It has been suggested that the increased intensity in the funneling illusion is not due to greater neuronal firing rates, but rather due to the recruitment of a wider distribution of neurons. Such recruitment in funneling could translate into a greater area of cortical activation that reflects a wider distribution of activated neurons or a greater amplitude of imaged reflectance, indicating greater neuronal firing activity and/or an increased number of recruited neurons. Alternatively, intensity could be encoded by a change in the spatial profile of activation, in which the ratio of the center to surround activation is increased.

We first examined the area of cortical activation in coding intensity. To obtain area measurements of an activation spot, we low-pass filtered and thresholded each image (Fig. 1, B, D, F, H, J, and L) and measured the area of a thresholded region (*8*, *10*, *11*). The threshold level was used uniformly across all images. The average area of single-digit activations in case 1 was 0.91 mm^2, and in case 2 the average was 0.66 mm^2. The percentage change of single-digit versus paired-digit activation areas was then calculated. The area of activation produced by adjacent (D3+D4) and nonadjacent (D2+D4) stimulation was smaller than the sum of the single-digit activation areas (case 1: adjacent 64% smaller, nonadjacent 44% smaller; case 2: adjacent 61% smaller, nonadjacent 55% smaller). We observed a reduction in area in all five adjacent pairs and all four nonadjacent pairs (Fig. 1Q). This result was not dependent on the precise threshold level used (*11*). In contrast to the predicted increases in activation area, two-finger stimulation leads to an overall reduction in activation area for both adjacent- and nonadjacent-digit pairs. Thus, activation area does not correlate with increased sensation magnitude.

We next examined the amplitude of activation in coding intensity. We first established that the magnitude of optical signal correlated with stimulus intensity by examining the optical responses to a constant stimulus intensity and a range of stimulus intensities. Stimulus amplitude was kept constant on D4 while the amplitude on D2 increased from low (148 mN) to medium (med, 296 mN) to high (592 mN) (Fig. 2, A and B). Consistent with the nature of the optical signal (*8*, *9*, *12*), the amplitude of the reflectance change was on the order of 0.1 to 1.0% and increased over a period of 2 to 3 s after the stimulus onset. Applying a constant stimulus intensity (on digit D4) resulted in similar signal amplitudes (blue curves) in each of four conditions (D4 alone, D4+D2 low, D4+D2 med, and D4+D2 high) (Fig. 2, C and E). Increasing stimulus intensity from low to medium to high (on digit D2) produced optical signals that increased in magnitude (Fig. 2, B and D). This systematic change in reflectance magnitude with stimulus intensity was observed in each case (n = 5, Fig. 2F).

We then evaluated the effect of two-digit stimulation on the amplitude of response at the locations of single-digit acti-

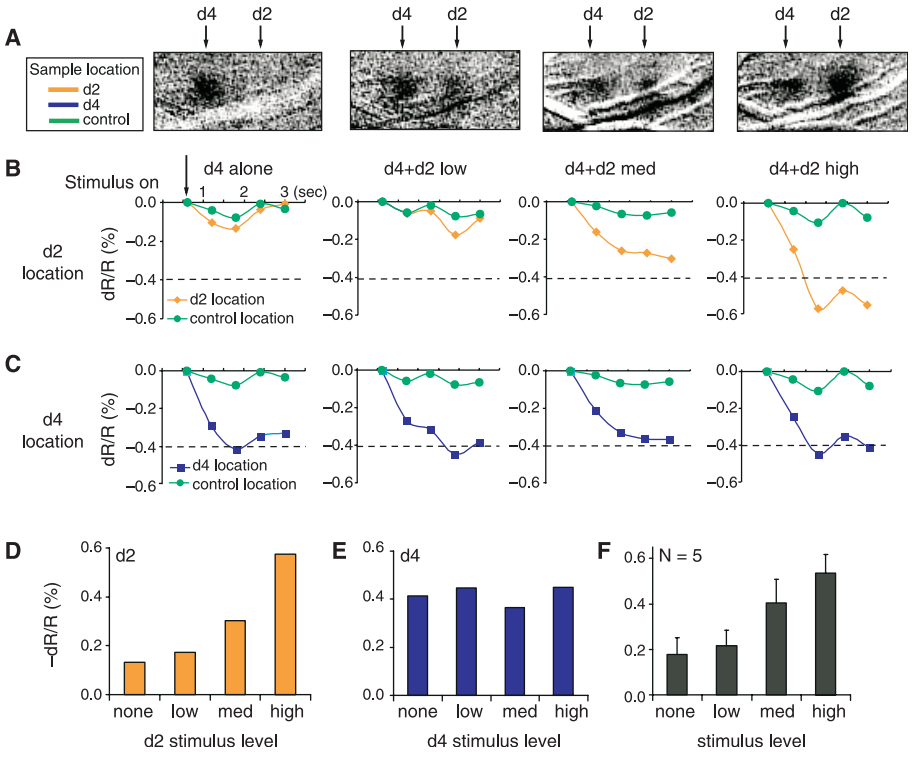

Fig. 2. Optical signal amplitude correlates with stimulus intensity. (**A**) Optical images in response to four stimulus conditions. A medium-intensity stimulus (296 mN) was applied to D4 and one of four intensity levels was simultaneously applied to D2 (none, 0 mN; low, 148 mN; med, 296 mN; and high, 592 mN; shown from left to right). (**B** and **C**) Reflectance change time courses. Increasing stimulus intensity on D2 produced increasing reflectance change [(B), orange], whereas a constant stimulus on D4 produced similar response amplitudes [(C), blue]. Little change occurred at a distant location [(B) and (C), green]. Downward arrow, stimulus onset. Peak amplitudes for D2 and D4 are plotted in (**D**) and (**E**), respectively. (**F**) Population data from five cases.

vation and at the merged location (Fig. 3A). Response amplitudes were examined at four locations: at the D3 and D4 activation sites, at a D34 location central to the other two, and at a distant control location. Stimulation of D4 alone produced activation at the D4 site and little activation elsewhere (Fig. 3B, top). Stimulation of D3 alone produced activation at the D3 site and some activation at the D34 and D4 sites (Fig. 3B, middle).

The predicted result of two-digit stimulation, obtained by the linear sum of the activations of D3 alone and D4 alone, was a U-shaped spatial activation profile (Fig. 3B, bottom, white bars). However, instead of a U-shaped profile, the measured activation profile (Fig. 3B, bottom, gray bars) was greatest at the central site. For all adjacent-digit pairs (Fig. 3C, $n = 5$) the mean magnitude of the signal decrease at the single-digit locations was 19.7%, and the increase at the central site was, on average, 33%. This center-weighted spatial profile resulted from two changes: (i) At the central site (D34), the signal amplitude increased compared with that of single-digit activations (e.g., compare the D3+D4 amplitude with that of D3 alone). (ii) At the single-digit sites (D3 and D4), the signal decreased compared with that of single-digit activations (e.g., compare the D3+D4 amplitude with that of D4 alone) (Fig. 3D).

A different activation profile was observed for nonadjacent-digit pairs. Figure 3E illustrates a case in which digits D2 and D4 were stimulated. D4 stimulation produced activation at the D4 site and negligible activation at the other sites (Fig. 3F, top). D2 stimulation produced activation at the D2 site and little activation elsewhere (Fig. 3F, middle). In contrast to adjacent-digit stimulation (Fig. 3, A to D), paired stimulation of D2 and D4 resulted in greater amplitudes at the D2 and D4 locations than at the center D3 or control locations (Fig. 3F, bottom, gray bars). The spatial profile of nonadjacent two-digit activation was similar in shape to the predicted linear summation of single digits (Fig. 3F, bottom, compare gray bars and white bars). However, the amplitude of two-digit stimulation was less than predicted at both single-digit sites. For all nonadjacent-digit pairs (Fig. 3G, $n = 4$) the mean decrease in signal at the single-digit locations was $33 \pm 7.6\%$ without affecting the signal size at the center (Fig. 3H). These findings are consistent with psychophysical observations that when two stimuli are spaced sufficiently far apart, they are perceived as two separate stimuli, each weaker in intensity than that of a single stimulus alone (*1*, *7*).

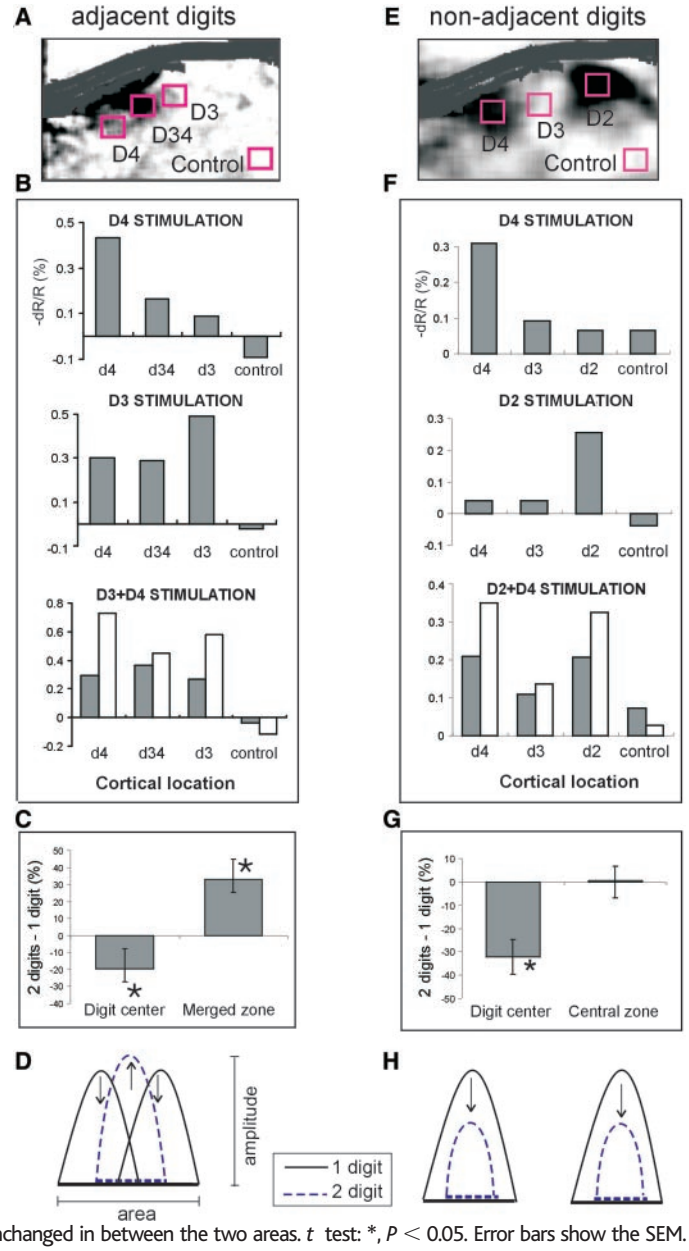

Fig. 3. Activation profiles of single- and two-digit stimulation. (**A** to **C**) Adjacent-digit (D3 and D4) stimulation (case 2). (A) Sampled regions indicated by boxes (D3, D34, D4, and control). (B) Signal amplitudes: response to single-digit (D4 alone, top; D3 alone, middle) and paired-digit (D3+D4, bottom, gray bars) stimulation. White bars in the bottom graph are the linear sum of single-digit amplitudes (top and middle). (C) Compared with single-digit stimulation, adjacent-digit stimulation produced decreases in activation at single-digit locations (left bar, $n = 10$) and increases at merged locations (right bar, $n = 5$). (**D**) Activations at single-digit locations (solid line) are reduced (downward arrows) and the activation at the merged location is increased (upward arrow). (**E** to **G**) Nonadjacent-digit (D2 and D4) stimulation (case 2). Samples from D2, D3, D4, and control locations. (G) Nonadjacent-digit stimulation produced decreased activation at digit centers (D2 and D4 locations, $n = 8$) and no activation change at the central zone (D3 location, $n = 4$). (**H**) Activations at single-digit locations (solid line) are reduced (downward arrows) but unchanged in between the two areas. *t* test: *, $P < 0.05$. Error bars show the SEM.

Stimulation of adjacent digits produced activation in the central merged zone comparable to the amplitude of single-digit activations. Even though no physical stimulus occurred at the merged site, the cortical response was comparable in size to that of an actual single-digit stimulus (single-digit mean $= 0.36 \pm 0.08\%$ reflectance amplitude, adjacent two-digit center zone mean $= 0.27 \pm 0.05\%$ reflectance amplitude, paired *t* test $P > 0.05$). However, this amplitude does not predict the heightened intensity of the funneling experience. It has been proposed that this intensity may occur as a result of a strengthening of a central stimulation site and a masking of peripheral sites (*6*, *7*). Consistent with, although distinct from, this suggestion, we report that the area of funneled activity is smaller relative to single-digit activation (Fig. 1Q), suggesting that the increased sensation intensity is encoded by a sharpened focus of cortical activation. We speculate that perceived tactile intensity is encoded by the differential response between neurons at the central site (increased amplitude) and those at nearby sites (decreased amplitudes).

That stimulation of multiple skin sites leads to a single cortical activation zone suggests that spatial perceptions are strongly dictated by central representations. Indeed, perception of a tactile stimulus can happen where no physical stimulus occurred. Although we cannot rule out subcortical contributions, the bulk of the evidence indicates a cortical locus. This study further suggests, contrary to previous studies (*13*, *14*), the presence of receptive fields in area 3b that, in certain contexts, span more than one digit (*15*–*17*). Such contextual influences from beyond the classical receptive field (*18*–*21*) are likely to be

determined by mechanisms dependent on intracortical distance, center and surround interactions, and cortical feedback.

References and Notes

1. G. von Bekesy, *Sensory Inhibition* (Princeton Univ. Press, Princeton, NJ, 1967).
2. E. P. Gardner, W. A. Spencer, *J. Neurophysiol.* **35**, 925 (1972).
3. I. Hashimoto, K. Yoshikawa, T. Kimura, *Neuroreport* **10**, 3201 (1999).
4. C. E. Sherrick, *Am. J. Psychol.* **77**, 42 (1964).
5. E. P. Gardner, J. M. Tast, *J. Neurophysiol.* **46**, 479 (1981).
6. E. P. Gardner, R. M. Costanzo, *J. Neurophysiol.* **43**, 420 (1980).
7. E. P. Gardner, W. A. Spencer, *J. Neurophysiol.* **35**, 954 (1972).
8. T. Bonhoeffer, A. Grinvald, in *Brain Mapping: The Methods*, A. W. Toga, J. C. Mazziotta, Eds. (Academic Press, London, 1996), pp. 55–97.
9. M. Sur, R. J. Nelson, J. H. Kaas, *J. Comp. Neurol.* **211**, 177 (1982).
10. L. M. Chen, R. M. Friedman, B. M. Ramsden, R. H. LaMotte, A. W. Roe, *J. Neurophysiol.* **86**, 3011 (2001).
11. Materials and methods are available as supporting material on *Science* Online.
12. M. Tommerdahl *et al.*, *J. Neurophysiol.* **80**, 3272 (1998).
13. R. J. Nelson, M. Sur, D. J. Felleman, J. H. Kaas, *J. Comp. Neurol.* **192**, 611 (1980).
14. T. P. Pons, J. T. Wall, P. E. Garraghty, C. G. Cusick, J. H. Kaas, *Somatosens. Res.* **4**, 309 (1987).
15. Y. Iwamura, M. Tanaka, M. Sakamoto, O. Hikosaka, *Exp. Brain Res.* **51**, 315 (1983).
16. T. M. McKenna, B. L. Whitsel, D. A. Dreyer, *J. Neurophysiol.* **48**, 289 (1982).
17. C. E. Schroeder, S. Seto, J. C. Arezzo, P. E. Garraghty, *J. Neurophysiol.* **74**, 722 (1995).
18. J. Allman, F. Miezin, E. McGuinness, *Annu. Rev. Neurosci.* **8**, 407 (1985).
19. V. Bringuier, F. Chavane, L. Glaeser, Y. Frégnac, *Science* **283**, 695 (1999).
20. M. K. Kapadia, G. Westheimer, C. D. Gilbert, *J. Neurophysiol.* **84**, 2048 (2000).
21. B. M. Ramsden, C. P. Hung, A. W. Roe, *Cereb. Cortex* **11**, 648 (2001).

22. We thank R. H. LaMotte for the use of his equipment and F. Healy for technical assistance.

Supporting Online Material

www.sciencemag.org/cgi/content/full/1087846/DC1
Materials and Methods
Fig. S1
Table S1
References

10 June 2003; accepted 27 August 2003
Published online 18 September 2003;
10.1126/science.1087846
Include this information when citing this paper.

Derepression of BDNF Transcription Involves Calcium-Dependent Phosphorylation of MeCP2

Wen G. Chen,[1,2] Qiang Chang,[3] Yingxi Lin,[1] Alexander Meissner,[3,4] Anne E. West,[1] Eric C. Griffith,[1] Rudolf Jaenisch,[3,4] Michael E. Greenberg[1,2]*

Mutations in *MeCP2*, which encodes a protein that has been proposed to function as a global transcriptional repressor, are the cause of Rett syndrome (RTT), an X-linked progressive neurological disorder. Although the selective inactivation of MeCP2 in neurons is sufficient to confer a Rett-like phenotype in mice, the specific functions of MeCP2 in postmitotic neurons are not known. We find that MeCP2 binds selectively to *BDNF* promoter III and functions to repress expression of the *BDNF* gene. Membrane depolarization triggers the calcium-dependent phosphorylation and release of MeCP2 from *BDNF* promoter III, thereby facilitating transcription. These studies indicate that MeCP2 plays a key role in the control of neuronal activity–dependent gene regulation and suggest that the deregulation of this process may underlie the pathology of RTT.

Methylation of DNA in vertebrates occurs preferentially on cytosine residues that occur in dinucleotides in which the cytosine residues are followed by guanine residues (CpGs). Methylated CpGs bind a variety of proteins (*1*). One of these proteins, the methyl-CpG binding protein 2 (MeCP2), has been implicated in long-term silencing of gene expression (*2–5*). Inactivating mutations in the *MeCP2* gene cause the majority of cases of Rett syndrome (RTT) (*6–8*), a human X-linked disorder characterized by arrested neurological development and subsequent cognitive decline (*9–11*). MeCP2 is abundantly expressed within the central nervous system, where its expression is highly enriched in postmitotic neurons (*12–14*). Although biochemical evidence is consistent with MeCP2 functioning as a global silencer of gene transcription (*3*), microarray analyses have failed to detect significant gene derepression in brains of *Mecp2* mutant mice (*15*). This finding, as well as the strong expression of MeCP2 in mature neurons and the neuronal phenotype of RTT patients, raised the possibility that MeCP2 may function as a selective regulator of neuronal gene expression.

Activity-dependent transcription underlies the ability of the nervous system to convert the effects of transient stimuli into long-term changes in brain function. Two classes of genes are regulated by neuronal activity–dependent calcium influx (*16*): immediate-early gene (IEG)–encoded transcription factors that mediate cellular responses to extracellular stimuli and genes selectively expressed in the nervous system that directly regulate neuronal development and synaptic plasticity. Of the neural-selective activity-dependent genes, that encoding brain-derived neurotrophic factor (BDNF) is among the most extensively studied. BDNF plays important roles in neuronal survival (*17*), development (*18*), and plasticity (*19*). *BDNF* is highly expressed in neurons, and its transcription is up-regulated dramatically by membrane depolarization in vitro (*18*, *20*, *21*) and by neuronal activity during kindling, induction of long-term potentiation (LTP), and associative learning (*22–24*). BDNF is encoded by a complex gene with four well-characterized promoters that give rise to at least eight different mRNAs (*25*) (Fig. 1A). Calcium influx through L-type voltage-sensitive calcium channels (L-VSCCs) activates *BDNF* promoter III, an effect that requires the action of at least three transcriptional activators [calcium-response factor, CaRF; upstream stimulatory factors, USFs; and calcium/cyclic adenosine monophosphate (cAMP)–responsive element binding protein, CREB] that bind to enhancer elements in promoter III (*21*, *26–28*). However, activation of CREB precedes the onset of transcription from *BDNF* promoter III (*21*), raising the possibility that a repressive mechanism may need to be relieved before the activation of transcription. The mechanisms by which *BDNF* transcription is repressed and then activated upon membrane depolarization are not yet clear. In this study, we report that, in the absence of neuronal activity, MeCP2 binds specifically to *BDNF* promoter III and functions as a negative regulator of *BDNF* expression. In response to neuronal activity–dependent calcium influx into neurons, MeCP2 becomes phosphorylated and is released from the *BDNF* pro-

[1]Division of Neuroscience, Children's Hospital, [2]Program in Biological and Biomedical Sciences, Harvard Medical School, Boston, MA 02115, USA. [3]Whitehead Institute for Biomedical Research, [4]Department of Biology, Massachusetts Institute of Technology, Cambridge, MA 02142, USA.

*To whom correspondence should be addressed. E-mail: Michael.Greenberg@tch.harvard.edu